Theoretical and experimental comparison of lag-based and time-based exponential moving average models of QT hysteresis

Vincent Jacquemet[1,2], **Hugo Gravel**[3], **Daniel Curnier**[3,4], **Alain Vinet**[1,2]

[1] Université de Montréal, Département de Pharmacologie et Physiologie, Institut de Génie Biomédical, Montréal, Canada; [2] Hôpital du Sacré-Coeur de Montréal, Centre de Recherche, Montréal, Canada; [3] Université de Montréal, Département de Kinésiologie, Montréal, Canada; [4] Centre Hospitalier Universitaire Sainte-Justine, Centre de Recherche, Montréal, Canada.

E-mail: `vincent.jacquemet@umontreal.ca`

Published in Physiol. Meas. (2017), vol. 38, no. 10, pp. 1885-1905

Abstract. In the electrocardiogram, adaptation of the QT interval to variations in heart rate is not instantaneous. Quantification of this hysteresis phenomenon relies on mathematical models describing the relation between the RR and QT time series. These models reproduce hysteresis through an effective RR interval computed as a linear combination of the history of past RR intervals. This filter depends on a time constant parameter that may be used as biomarker. The most common hysteresis model is based on an autoregressive filter with an impulse response that decreases exponentially with the beat number (lag-based model). Recognizing that the QT time series is unevenly spaced, we propose two exponential moving average filters (time-based models) to define the effective RR interval: one with an impulse response that decreases exponentially with time in seconds, and one with a step response that relaxes exponentially with time in seconds. These two filters are neither linear nor time-invariant. Recurrence formulas are derived to enable efficient implementation. Application to clinical signals recorded during tilt table test, exercise and 24h Holter demonstrates that the three models perform similarly in terms of goodness-of-fit. When comparing the hysteresis time constant in two conditions with different heart rates, however, the time-based models are shown to reduce the bias on the hysteresis time constant caused by heart rate acceleration and deceleration.

1. Introduction

The QT interval of the electrocardiogram (ECG) is a descriptor of ventricular repolarization. The adaptation of the QT interval in response to a sudden change in heart rate is not instantaneous. It occurs with a delay, thus creating a hysteresis phenomenon (Lau et al. 1988, Malik et al. 2008). QT hysteresis is believed to provide

potential biomarkers to predict arrhythmic mortality in survivors of acute myocardial infarction (Pueyo et al. 2004), the risk of torsade de pointes (Trost 2008), and the occurrence of ventricular tachycardia (Chen and Trayanova 2012, Chen et al. 2013) and myocardial ischemia (Lauer et al. 2006). Differences in QT hysteresis have been observed in relation to the long QT syndrome (Krahn et al. 1997, Krahn et al. 2002, Gao et al. 2007, Wong et al. 2010, Chattha et al. 2010), coronary artery disease (Zhang et al. 2014) and hypertension (Halamek et al. 2010). These studies often used treadmill or ergometer exercise tests to induce changes in heart rate. QT hysteresis measures may be combined with standard QT variability indices (Berger 2003, Dobson et al. 2013).

Quantifiers of QT hysteresis include direct measurement of QT time course, often during atrial pacing (Lau et al. 1988, Grom et al. 2005), differences in QT interval between heart rate acceleration and deceleration (Krahn et al. 1997, Chauhan et al. 2002, Lewis and Short 2006), the area of the QT-RR loop (Sarma et al. 1987, Lauer et al. 2006, Pelchovitz et al. 2012), and, more recently, measures derived from subject-specific modeling of QT-RR dynamics (Pueyo et al. 2003, Halamek et al. 2007, Jacquemet et al. 2011).

Mathematical models of the relation between the RR intervals and the QT intervals have been developed in order to define parameters describing the time constant of QT hysteresis (Gravel et al. 2017). These models typically rely on an effective RR interval computed as a linear combination of the history of past RR intervals (Pueyo et al. 2003). The weights of past RR intervals decrease with time, either represented by the number of beats (lag-based approach) or the time elapsed in seconds (time-based approach). Accounting for QT hysteresis has been shown to reduce the variability of the corrected QT interval (Malik et al. 2008, Jacquemet et al. 2011) and improve its accuracy in thorough QT pharmacological studies (Malik et al. 2009*a*, Malik et al. 2009*b*, Malik et al. 2016).

Nearly all studies so far quantified the hysteresis time constant in beats because of its convenient link to digital filters and system identification theory (Halamek et al. 2010, Jacquemet et al. 2011). Malik et al. (2008) compared the two approaches in daytime recordings in normal subjects and the observed differences were small. Indeed, as long as the RR interval distribution is unimodal, the mean RR serves as a factor to translate the time constant in beats into seconds. In the case of a bimodal RR distribution, however, when two distinct conditions associated with different heart rates are included and compared, the link between lag-based and time-based approaches becomes unclear and a time constant in seconds seems both theoretically preferable and physiologically relevant.

This paper presents a mathematical formulation and an efficient implementation of time-based approaches with exponentially-decaying weights. The emphasis is on the identification of potential heart rate-dependent biases that may affect the hysteresis time constant. In addition to theoretical analysis, the clinical application to intra-subject comparison of QT hysteresis is evaluated.

2. Material and methods

2.1. Data collection

ECG Holter data of a total of 139 normal subjects from three different protocols were collected.

Eleven normal subjects underwent a tilt-table test (Hamidi et al. 1997). The tilt-table protocol, 70 min in duration, consisted in four 10 min periods in supine position separated by three 10 min periods in orthostatic positions at 90°, 70° and 45° successively. Three-lead orthogonal ECG were recorded.

Sixty normal subjects underwent an exercise test comprising 10 repetitions of 4 min of exercise followed by 4 min of recovery. Exercise intensity varied between 30% and 60% of peak VO2. Standard 12-lead ECG were recorded.

ECG signals of a thorough QT study with crossover design (database "Thorough QT Study #2" E-HOL-12-0140-008) were obtained from the Telemetric and Holter ECG Warehouse (Rochester, NY). The 24h-duration standard 12-lead ECG recorded in 68 normal subjects during placebo delivery were used.

An ECG fiducial point detector (Dubé et al. 1988) was applied to the vector magnitude signal (root mean square of the three ECG leads) to identify the R, Q onset and T offset markers (Jacquemet et al. 2011). The resulting RR and QT time series were manually validated. Artifacts, signal saturation, premature ventricular contractions, ventricular arrhythmias and noisy or unreliably detected T waves were eliminated from the list of valid beats.

The set of valid beats was manually partitioned into two subsets associated with faster and slower heart rates: in the tilt-test group the subsets were supine position (heart rate deceleration) and orthostatic positions (acceleration); in the exercise group, the subsets were exercise and recovery; in the Holter 24h group, the subsets were day and night.

2.2. QT-RR modeling

In a sequence of N beats, the time instant of the i-th R wave is denoted by t_i and the QT interval of the i-th beat by QT_i. The RR interval preceding beat i is defined as $RR_i = t_i - t_{i-1}$. The zero-th beat, at time t_0, is used solely to define RR_1. This gives two time series RR_i and QT_i of length N.

A QT-RR model is described by a static QT-RR relationship and a hysteresis model (Pueyo et al. 2004, Jacquemet et al. 2011)

$$QT_i = f_\gamma(\overline{RR}_i) + \epsilon \quad , \tag{1}$$

where ϵ is the modeling error. The static QT-RR relationship is a function $f_\gamma(RR)$ depending on a set of parameters γ. We will use the shifted power function

$$f_\gamma(RR) = \gamma_1 + \gamma_2 RR^{\gamma_3} \tag{2}$$

with $\gamma = (\gamma_1, \gamma_2, \gamma_3)$. This family of curves notably includes the Bazett's and Fridericia's formulas and enables the adjustment of QT-RR curvature (Malik et al. 2012).

A hysteresis model provides a definition of the effective RR interval ($\overline{RR}_i$) as a function of the history of preceding RR intervals ($RR_j,\ j \leq i$), following the general linear form

$$\overline{RR}_i = \frac{\sum_{j \leq i} w_{i,j} RR_j}{\sum_{j \leq i} w_{i,j}} \quad , \tag{3}$$

where $w_{i,j}$ is the weight of beat j in the calculation of $\overline{RR}_i$. In the general case, computing the $\overline{RR}$ time series requires $\mathcal{O}(N^2)$ arithmetic operations. By restricting $w_{i,j}$ for each i to L non-zero values ($j = i-L+1, \ldots, i-1, i$), the number of operations is reduced to $\mathcal{O}(NL)$ as in Malik et al. (2008). Since L is often of the order of 300 (Pueyo et al. 2003) and N may be as large as 100,000 (Holter 24h), it is desirable to seek formulas that can be computed in $\mathcal{O}(N)$ operations (see Appendix A).

The weights are functions $w_{i,j}(\tau)$ of a time constant τ expressing the adaptation time for the QT interval after sudden change in heart rate. Determination of the parameters γ and τ based on the RR and QT time series is performed by optimizing the mean square prediction error

$$E^2_{RMS}(\tau, \gamma; \mathcal{V}) = \frac{1}{|\mathcal{V}|} \sum_{i \in \mathcal{V}} \left(QT_i - f_\gamma(\overline{RR}_i) \right)^2 \quad . \tag{4}$$

The subset $\mathcal{V} \subset \{1, \ldots, N\}$ lists the valid beats after exclusion of artifacts, ectopic beats and arrhythmias, and can be used for parameter optimization over a set of time segments (e.g. exercise or recovery). $|\mathcal{V}|$ is the number of beats in $\mathcal{V}$. The numerical techniques we used for minimizing $E^2_{RMS}(\tau, \gamma; \mathcal{V})$ for a given $\mathcal{V}$ are presented in Jacquemet et al. (2011). These methods are comparable to the previous works of Halamek et al. (2010) and Pueyo et al. (2004).

2.3. Exponential hysteresis models

Two exponential formulas for the weights of the hysteresis model have been proposed, the lag-based (or interval-based) exponential model

$$w_{i,j} = e^{-(i-j)/\tau_b} \tag{5}$$

where the time constant τ_b is expressed in beats, and the time-based exponential model

$$w_{i,j} = e^{-(t_i - t_j)/\tau_s} \tag{6}$$

where the time constant τ_s is in seconds. Recall that $w_{i,j}$ is defined only for $j \leq i$, so that $0 < w_{i,j} \leq 1$.

These time constants are related to the hysteresis parameters λ_l and λ_T defined in Malik et al. (2008): $\lambda_l = L/\tau_b$ and $\lambda_T = L\,\langle RR \rangle / \tau_s$ where L is the window duration in beats and $\langle RR \rangle$ is the mean RR interval over the L preceding beats. As a result, $\tau_s/\tau_b = \langle RR \rangle\, \lambda_l/\lambda_T$. An advantage of our formulation is that the parameters τ_b and τ_s are not based on a fixed-length sliding window, so they do not depend on L.

The formula (3) for the effective RR defines a filter acting on an unequally spaced signal $(t_i, x_i)_{i=1,\dots,N}$ whose value at time t_i is x_i. Three variants of the filter were used. Their pseudocode implementation is provided in Table 1, the mathematical justification of the algorithms is presented in Appendix A and the derivation of their properties is shown in Appendix B. The first-order autoregressive filter (AR1) has lag-based exponential weights (5) and an exponential step function (which means an exponential adaptation to a sudden change in heart rate). The exponential moving average filter (EMA) has time-based exponential weights (6) but only an approximate exponential step function. The equivalent EMA filter (EMAeq) is an adjustment of the AR1 algorithm that makes it similar to EMA. It has an exact exponential step function but the decay of its weights is only approximately exponential (and not even monotonic).

Each of the filters AR1, EMA and EMAeq defines a hysteresis model (called AR1, EMA and EMAeq models hereafter) by applying the filter to the RR time series, i.e. with $x_{i+1} = t_{i+1} - t_i = RR_{i+1}$ in Table 1. The AR1 model remains a simple linear time-invariant filter of the RR time series. In contrast, in the EMA and EMAeq models, the weights of the filter are correlated with the values of the time series to be filtered because $c = e^{-RR_{i+1}/\tau}$ in the notations of Table 1. As a result, these filters are neither linear nor time-invariant since the weights are nonlinear functions of the RR values.

2.4. Adaptation time

Instead of time constants, time to 90% of QT adaptation ($T_{0.9}$) is sometimes reported (Gravel et al. 2017), in particular when the hysteresis model may not be exponential. Under the assumption that QT adaptation is exponential, this measure of hysteresis should correspond to $\tau \log(10) \approx 2.3\,\tau$.

The time to β% of $\overline{RR}$ adaptation (denoted by $\overline{T}_\beta$) will also be calculated. As long as the static QT-RR relation f_γ is linear, $T_{0.9} = \overline{T}_{0.9}$, i.e. the time constants of QT adaptation and $\overline{RR}$ adaptation are the same. Otherwise, QT adaptation is non-linearly related to $\overline{RR}$ adaptation. If a subject in condition A with initial RR interval RR_A changes to condition B with final RR interval RR_B, then $T_{0.9} = \overline{T}_\beta$ where

$$\beta = \frac{f_\gamma^{-1}(0.1 f_\gamma(RR_A) + 0.9 f_\gamma(RR_B)) - RR_A}{RR_B - RR_A} \quad . \tag{7}$$

If heart rate is assumed to be stable in conditions A and B and if the transition is abrupt, the time to $\overline{RR}$ adaptation can be calculated explicitly for all three hysteresis models from the step functions (B.2), (B.4) and (B.6) derived in Appendix B:

$$\overline{T}_\beta = \begin{cases} -\tau_b\, RR_B\, \log(1-\beta) & \text{AR1 model} \\ \tau_s\, \log\left(1 + \frac{\beta}{1-\beta} \cdot \frac{RR_B}{RR_A}\right) & \text{EMA model} \\ -\tau_s\, \log(1-\beta) & \text{EMAeq model} \end{cases} \tag{8}$$

With the AR1 model, the adaptation time $\overline{T}_\beta$ depends on the final RR interval. In a QT-RR loop following this model, QT adaptation is faster during heart rate acceleration (RR $\downarrow$) and slower during deceleration (RR $\uparrow$). With the EMA model, if $RR_A \approx RR_B$,

Inputs:	$(t_i)_{i=0,\dots N}$ (time series)
	$(x_i)_{i=1,\dots N}$ (value of the signal)
	τ_b or τ_s (time constant)
Output:	$(\bar{x}_i)_{i=1,\dots N}$ (filtered signal)
AR1:	$c := \exp(-1/\tau_b)$
	$\bar{x}_1 := x_1$
	`for` $i := 1$ `to` $N-1$
	$\quad \bar{x}_{i+1} := (1-c)x_{i+1} + c\,\bar{x}_i$
	`end`
EMA:	$c := \exp(-(t_1 - t_0)/\tau_s)$
	$a := x_1/(1-c)$
	$b := 1/(1-c)$
	$\bar{x}_1 := x_1$
	`for` $i := 1$ `to` $N-1$
	$\quad c := \exp(-(t_{i+1} - t_i)/\tau_s)$
	$\quad a := x_{i+1} + c\,a$
	$\quad b := 1 + c\,b$
	$\quad \bar{x}_{i+1} := a/b$
	`end`
EMAeq:	$\bar{x}_1 := x_1$
	`for` $i := 1$ `to` $N-1$
	$\quad c := \exp(-(t_{i+1} - t_i)/\tau_s)$
	$\quad \bar{x}_{i+1} := (1-c)x_{i+1} + c\,\bar{x}_i$
	`end`

Table 1. Pseudocode algorithms for the three exponential filters AR1 (lag-based), EMA (time-based; exponential weights) and EMAeq (time-based; exponential step function). The operator := denotes assignment. For AR1, τ_b is in beats and for EMA and EMAeq, τ_s is in seconds. In the case of the RR time series, $x_{i+1} = t_{i+1} - t_i$. For the EMA algorithm, if t_0 is unknown, $t_1 - t_0$ may be replaced with $t_2 - t_1$ in the initialization of c.

we still have $\overline{T}_\beta = -\tau_s \log(1-\beta)$, but otherwise a correction factor must be applied to interpret τ_s as an adaptation time. QT adaptation is always slower during deceleration than acceleration, as with the AR1 model. In contrast, with the EMAeq model, the adaptation time is the same for both heart rate acceleration and deceleration. In this case, the subject-specific τ_s value is a measure of $\overline{RR}$ adaptation time.

2.5. Shift of the QT-RR relation

Time-invariant linear filters such as the AR1 model have the property that the mean (over the whole signal) effective RR interval is equal to the mean RR interval. The EMA and EMAeq models are neither time-invariant (unless the RR time series is constant) nor linear (the factor c depends on RR). A difference between the mean RR and mean effective RR may lead to a horizontal shift of the $(\overline{RR}, QT)$ cloud of points that would modify the predicted QT interval and thus the QTc.

The amplitude of the bias $\mathsf{E}[\overline{RR}_i - RR_i]$, where $\mathsf{E}[X]$ is the expectation of a random variable X, can be estimated under the assumption that the RR intervals are

independent and normally distributed with mean μ and variance σ^2 (Appendix C):

$$\mathsf{E}[\overline{RR}_i - RR_i] = \begin{cases} 0 & \text{AR1 model} \\ \dfrac{\sigma^2}{2\tau_s} + \mathcal{O}(\tau_s^{-2}) & \text{EMA model} \\ \dfrac{\sigma^2}{\mu} + \mathcal{O}(\tau_s^{-1}) & \text{EMAeq model} \end{cases} \tag{9}$$

For reasonable parameter values $\mu = 900$ ms, $\sigma = 60$ ms and $\tau_s = 50$ s, the bias with the EMAeq model is 4 ms. With a QT-RR slope of 0.2, this decreases the QT at a given $\overline{RR}$ by 0.8 ms. With the EMA model, the bias is 0.036 ms which is negligible for practical purpose.

2.6. Bias-corrected estimate of the QTc

The QTc is the QT interval at a stable RR interval of 1000 ms. In other words, QTc $= f_\gamma(\overline{RR})$ where $RR = 1000$ ms and f_γ is the individualized QT-RR relation. Usually, this means that QTc $= f_\gamma(1000)$, but for example in the case of the EMAeq model, the $\overline{RR}$ is biased in the presence of RR fluctuations. Instead, in first approximation, the QT-RR function is evaluated at the mean $\overline{RR}$ for $\mu = 1000$ ms, giving the $\overline{RR}$ bias-corrected QTc

$$\text{QTcb} = f_\gamma\left(1000 + \mathsf{E}[\overline{RR}_i - RR_i]\right) \ , \tag{10}$$

where the expectation is estimated directly from the RR and $\overline{RR}$ time series. This assumes that the shift of the QT-RR relation (fitted to the whole recording) is uniform over all RR intervals. In the case of the EMAeq model applied to the random Gaussian RR fluctuations of the Appendix C, this assumption is supported by the fact that $\mathsf{cov}(\overline{RR}_i - RR_i,\ RR_i) = \mathcal{O}(\tau^{-1})$, so the bias is weakly correlated to the RR interval.

2.7. Intra-subject variations in QT hysteresis

The parameters that minimize $E^2_{RMS}(\tau, \gamma; \mathcal{V})$, where $\mathcal{V}$ is the set of all valid beats of the recording, will be called $\hat{\tau}_{\text{global}}$ and $\hat{\gamma}_{\text{global}}$. The parameter τ can represent either τ_b or τ_s.

Now assume that the recording is divided into at least two subsets of beats $\mathcal{S}_k \subset \mathcal{V}$, $k = A, B, \ldots$, representing different physiological conditions or protocol time points (e.g. heart rate acceleration vs deceleration, supine vs standing position, exercise vs recovery). We would like to test the (null) hypothesis that QT hysteresis is the same in these different states. The static QT-RR relation will be assumed to remain constant in the whole recording ($\gamma = \hat{\gamma}_{\text{global}}$). The consistency of this assumption can be tested a posteriori by looking at the structure of the residuals. The rationale for this assumption is that the static QT-RR relationship cannot be estimated separately in the upper and the lower arm of a QT-RR loop. When isolated, the upper arm might indeed be reproduced without hysteresis by shifting upwards the QT-RR relationship. Also, if heart rate is significantly different in the segments $\mathcal{S}_k$, extrapolation of the QT-RR

relation beyond the range of RR used for the fitting procedure may be inaccurate (Vinet et al. 2017).

The estimated hysteresis time constant $\hat{\tau}_k$ associated with the state $\mathcal{S}_k$ is obtained by minimizing the mean square error $E^2_{RMS}(\tau, \hat{\gamma}_{\text{global}}; \mathcal{S}_k)$ over all positive values of τ. Practically, the error is minimized in the interval from 1 to 120 sec. or beats using an approach based on golden section search and parabolic interpolation. In order to get a sense of the uncertainty on $\hat{\tau}_k$, the range of τ over which the error varies by less than 1% is calculated. For that purpose the equation $E_{RMS}(\tau, \hat{\gamma}_{\text{global}}; \mathcal{S}_k) = 1.01 \cdot E_{RMS}(\hat{\tau}_k, \hat{\gamma}_{\text{global}}; \mathcal{S}_k)$ is solved using the regula falsi algorithm in the intervals $[1, \hat{\tau}_k]$ and $[\hat{\tau}_k, 120]$. In the figures, the resulting interval $[\hat{\tau}_k^-, \hat{\tau}_k^+]$ will be displayed as error bar. The absolute uncertainty $\Delta\hat{\tau}_k$ will be defined as half the length of the interval, i.e. $\Delta\hat{\tau}_k = (\hat{\tau}_k^+ - \hat{\tau}_k^-)/2$. The relative uncertainty will be computed as $\Delta\hat{\tau}_k/\hat{\tau}_k$.

3. Results

3.1. Characterization of exponential moving average filters

To illustrate and compare the characteristics of the three filters AR1, EMA and EMAeq, a synthetic example was generated, in which the sequence (t_i) was random with $t_i - t_{i-1}$ uniformly distributed around a mean that suddenly changes at $t = 3.6$ in arbitrary unit (Fig. 1). The signal x_i to be filtered is a step function with value 1 within a time interval [1.2,5.1] and 0 otherwise. Note that in contrast with the application to RR intervals, this signal is independent from the times t_i. The time constant τ_s was set to 0.8 and τ_b to $\tau_s/\langle t_i - t_{i-1}\rangle$, where the average $\langle\cdot\rangle$ was calculated over the entire signal.

Left panels of Fig. 1 show the resulting filtered signals (calculated using the formulas from Appendix A) compared to the theoretical exponential adaptation with a time constant of τ_s. The AR1 filter is not able to account for local changes in heart rate, so it either underestimates or overestimates adaptation time. The EMA filter approximates well exponential adaptation. The EMAeq filter gives an exact step response.

In unevenly spaced time series, the weights of the filter are not stationary. The weights expressing cardiac memory at time $t = 5.2$ are displayed in the right panels of Fig. 1. The weight of the k-th beat was computed as the response at time $t = 5.2$ of a unit impulse initiated at the time of the k-th beat. The results demonstrate that the lag-based filter AR1 deviates from exponential weights when expressed as a function of time and not lag. The EMA filter has by construction exact exponential weights. The EMAeq has approximately exponential weights with some significant fluctuations.

3.2. Goodness-of-fit

The subject-specific parameters γ (describing the static QT-RR curve; Eq. (2)) and τ (hysteresis time constant) were optimized for each subject and each method (AR1, EMA and EMAeq) over the whole recordings. Table 2 summarizes the goodness-of-fit in the three groups of subjects. The time constants τ_b of the AR1 model were converted

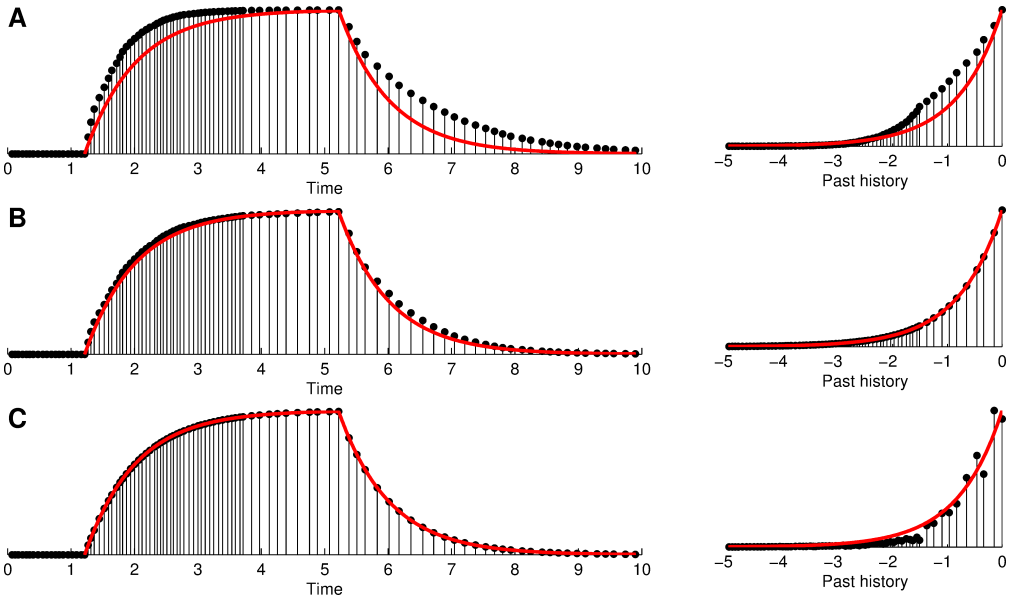

Figure 1. Step response (left panels) and weights of the history of previous RR intervals (right panels) expressed as a function of time for (A) the AR1 model, (B) the EMA model and (C) the EMAeq model. The red solid curves shows exact exponential adaptation.

into seconds by multiplying by the mean RR over the whole recording. The root mean square (RMS) error was similar for all methods. The AR1 method was slightly better during exercise (Friedman test $p < 0.001$).

The time constants τ differed slightly between the methods (in each of the three protocols, Friedman test $p < 0.01$), but the uncertainty intervals of the three methods had a common intersection in all subjects. The relative uncertainties $\Delta\tau/\tau$ were almost identical and ranged from 10% to 30%, confirming that the global RMS error is not very sensitive to the parameter τ (Vinet et al. 2017).

3.3. QT-RR curve and QTc estimation

Instead of comparing the three components of γ, the fitted QT-RR curves were compared directly by calculating the maximum QT difference (in absolute value) between two curves (QTdist in ms). The reference QT-RR curve was the one fitted using the AR1 model and the maximum was computed over the range of effective RR obtained from the AR1 model. The maximum distance was typically of the order of 1 ms (Table 3). This resulted in a QTc value $f_\gamma(1000)$ that was shorter with the EMA and EMAeq models than with the AR1 model. Part of these differences in QTc were due to the RR bias $\mathsf{E}[\overline{RR}_i - RR_i]$. This bias ($\text{bias}_{RR}^{exp}$) was zero with the AR1 model, < 1 ms with the EMA model, and of the order of 5-6 ms with the EMAeq model (Table 3). The theoretical value of the bias (bias_{RR}^{theor}) computed from (9) gave similar numbers. This enabled a bias correction of the QTc (QTcb in Table 3) that improved the consistency between

Model	RMS error (ms)	τ (sec)	$\Delta\tau/\tau$
	Tilt test ($n = 11$)		
AR1	2.92 ± 0.60	28.8 ± 6.4	0.10 ± 0.03
EMA	2.93 ± 0.61	28.5 ± 6.5	0.10 ± 0.03
EMAeq	2.92 ± 0.64	29.6 ± 6.9	0.10 ± 0.03
	Exercise test ($n = 60$)		
AR1	7.52 ± 1.73	41.1 ± 8.7	0.13 ± 0.05
EMA	7.73 ± 1.70	39.8 ± 9.5	0.13 ± 0.05
EMAeq	8.01 ± 1.71	36.8 ± 9.2	0.14 ± 0.04
	Holter 24h ($n = 68$)		
AR1	7.24 ± 1.46	72.4 ± 16.4	0.29 ± 0.06
EMA	7.28 ± 1.46	68.8 ± 16.7	0.29 ± 0.07
EMAeq	7.20 ± 1.50	65.8 ± 15.4	0.29 ± 0.07

Table 2. Root mean square (RMS) error of QT prediction, the parameter τ and its relative uncertainty $\Delta\tau/\tau$ shown for the three groups.

Model	QTdist (ms)	ΔQTc (ms)	bias_{RR}^{exp} (ms)	bias_{RR}^{theor} (ms)	ΔQTcb (ms)
		Tilt test ($n = 11$)			
EMA	0.6 ± 0.3	-0.2 ± 0.5	0.1 ± 0.0	0.1 ± 0.0	-0.2 ± 0.5
EMAeq	1.1 ± 0.6	-1.1 ± 0.6	5.7 ± 2.9	4.7 ± 2.9	-0.1 ± 0.4
		Exercise test ($n = 60$)			
EMA	1.4 ± 0.6	-1.0 ± 1.0	-0.4 ± 0.4	0.1 ± 0.0	-1.0 ± 1.0
EMAeq	2.2 ± 1.2	-2.0 ± 1.3	5.6 ± 2.7	6.9 ± 3.4	-1.4 ± 1.2
		Holter 24h ($n = 68$)			
EMA	0.7 ± 0.3	-0.2 ± 0.3	0.0 ± 0.0	0.0 ± 0.0	-0.2 ± 0.3
EMAeq	1.8 ± 1.2	-1.1 ± 0.5	6.2 ± 3.6	6.2 ± 3.6	0.0 ± 0.5

Table 3. Comparison of the QT-RR curves of the EMA and EMAeq models with the AR1 model as reference.

the methods, notably in Holter 24h data where RR intervals distribution is closer to a Gaussian as hypothesized in our simplified model of random fluctuations of heart rate. Large RR fluctuations and bimodal RR distribution during the exercise protocol made the bias correction less accurate in that case.

3.4. Intra-subject comparison of QT hysteresis

In the following subsections, the capabilities and limitations of the three methods to detect intra-subject differences in QT hysteresis will be evaluated. In each subject, two conditions were distinguished, corresponding to two distinct subsets of beats: heart rate acceleration vs deceleration in the tilt test group, exercise vs recovery in the exercise test group, and day vs night in the Holter 24h group. Repetitions, e.g. the time segments of exercise with different intensities, were pooled. These conditions were associated with different heart rates (Table 4). We will test the hypothesis that QT hysteresis is different in each condition.

Protocol	Condition	mean RR (ms)	mean QT (ms)	# beats
Tilt test	Acceleration	718.8 ± 71.4	322.8 ± 17.8	2444 ± 233
	Deceleration	978.0 ± 145.6	361.6 ± 25.9	1882 ± 293
Exercise test	Exercise	519.0 ± 49.9	303.2 ± 20.7	4438 ± 583
	Recovery	683.0 ± 93.9	322.1 ± 24.8	3428 ± 569
Holter 24h	Day	865.6 ± 95.1	359.9 ± 23.5	61227 ± 7853
	Night	989.5 ± 106.5	389.0 ± 26.7	26034 ± 5551

Table 4. Mean RR and QT intervals in each condition for the three groups. The standard deviation refers to inter-subject variability.

Protocol	Curvature (s^{-1})	Condition	$T_{0.9}/\overline{T}_{0.9}$
Tilt test	−0.10 ± 0.19	Acceleration (RR ↓)	1.02 ± 0.05
		Deceleration (RR ↑)	0.98 ± 0.05
Exercise test	−0.82 ± 0.30	Exercise (RR ↓)	1.09 ± 0.04
		Recovery (RR ↑)	0.91 ± 0.04
Holter 24h	0.13 ± 0.22	Day (RR ↓)	0.98 ± 0.03
		Night (RR ↑)	1.02 ± 0.03

Table 5. Ratio of the time constants of QT adaptation ($T_{0.9}$) and $\overline{RR}$ adaptation ($\overline{T}_{0.9}$) for heart rate acceleration (RR ↓) and deceleration (RR ↑) in the intervals documented in Table 4. Curvature refers to the maximal curvature of the QT-RR curve (fitted with the AR1 model) in the same RR range.

3.5. Bias caused by the non-linearity of the QT-RR relation

Equation (7) shows that QT and $\overline{RR}$ adaptation do not have the same time constant unless the static QT-RR relation is linear. Assuming exponential relaxation (B.1) of the $\overline{RR}$ interval, the ratio of the time constants of QT and RR reads:

$$\frac{T_{0.9}}{\overline{T}_{0.9}} = \frac{\overline{T}_{\beta}}{\overline{T}_{0.9}} = \frac{\log(1-\beta)}{\log(0.1)} \ , \tag{11}$$

where β is computed from the initial and final RR intervals and QT-RR relation using (7).

The non-linearity of the QT-RR relation was quantified using the curvature defined as $\kappa = f''_\gamma(RR)/(1+f'_\gamma(RR)^2)^{3/2}$. Positive curvature means concave up, negative concave down, and zero corresponds to a straight line. The most extreme (positive or negative) curvature value was documented for each subject. The extremum was computed over the RR range from the mean RR during one condition (e.g. exercise) to the mean RR during the other condition (e.g. recovery).

To estimate the impact of non-linearity, the ratio (11) was computed for increasing and decreasing heart rates with starting and final RR intervals given in Table 4. As shown in Table 5, the ratio $T_{0.9}/\overline{T}_{0.9}$ depends on the curvature of the QT-RR curve in the RR range considered. In concave down QT-RR relations, the time constant of QT adaptation is prolonged as compared to that of $\overline{RR}$ during heart rate acceleration and shortened during deceleration. The effect is reversed in concave up (convex) QT-RR relations. Even if the time constant of $\overline{RR}$ were exactly the same during exercise and

recovery, the time constant of QT adaptation would differ by up to 18%, due solely to the effect of QT-RR non-linearity. Note that the curvature obtained depends on the range of RR available for parameter optimization: during exercise the range is wider so the resulting QT-RR curve exhibits saturation at higher heart rate, while at rest the relation is close to linear and the non-linearity effect is of the order of ±2%.

Since $T_{0.9}$ depends explicitly on the range of RR and on the QT-RR relation, it appears that $\overline{T}_{0.9}$ is a more intrinsic parameters. The remaining will focus on this parameter.

3.6. Comparison of hysteresis models

The time constant τ was extracted in each subject using the three models successively for the two conditions with increasing or decreasing heart rate (e.g. exercise and recovery) and for the whole recording (i.e. global value of τ). The resulting values are compared in the left panels of Fig. 2. The time constants τ_b in beats obviously differed from the τ_s in seconds, reflecting a large inter-patient variability in heart rates. The two time constants τ_s in seconds were more consistent, but τ_s(EMA) was longer than τ_s(EMAeq) in conditions with faster heart rates and shorter in conditions with slower heart rates.

These discrepancies motivated the comparison of $\overline{RR}$ adaptation time $\overline{T}_{0.9}$ (right panels of Fig. 2). For the AR1 model, $\overline{T}_{0.9}$ was computed using (8) where $\beta = 0.9$ and RR_B was the (subject-specific) mean RR among the beats from which τ_b was extracted. For the EMA model applied to one condition, formula (8) was used; RR_A was the mean RR among the beats *not* considered. For example, to compute $\overline{T}_{0.9}$ during exercise, RR_B = mean RR during exercise and RR_A = mean RR during recovery. For the EMA model on the whole recording and for all applications of the EMAeq model, $\overline{T}_{0.9}$ was set to $\tau_s \log(10)$. As a result of these corrections, the consistency of $\overline{T}_{0.9}$ between the models was improved as compared to τ.

3.7. Intra-subject differences in time constant

In each protocol, the intra-subject variations of QT hysteresis time constant was studied in the two conditions associated with different mean heart rates. Figure 3 shows a Bland-Altman plot of the time constants τ in beats or in seconds for both conditions. During tilt test, the time constant was shorter during heart rate deceleration. The difference was significant with the AR1 model (paired t-test $p < 0.01$) and the EMA model ($p < 0.05$) but disappeared with the EMAeq model (panel A). During Holter 24h, the variability was large and no difference was found except using the EMAeq model, where the time constant was longer at night (panel C). During exercise test, the time constant was significantly longer during recovery whatever the model (panel B).

Since these differences may simply be caused by changes in heart rate, $\overline{T}_{0.9}$ was computed with correction for heart rate as in the previous subsection. Figure 4 shows the same plots as Fig. 3 for $\overline{T}_{0.9}$. The differences during tilt test disappeared (panel A), demonstrating that the differences observed in Fig. 3 were likely due to a bias of the

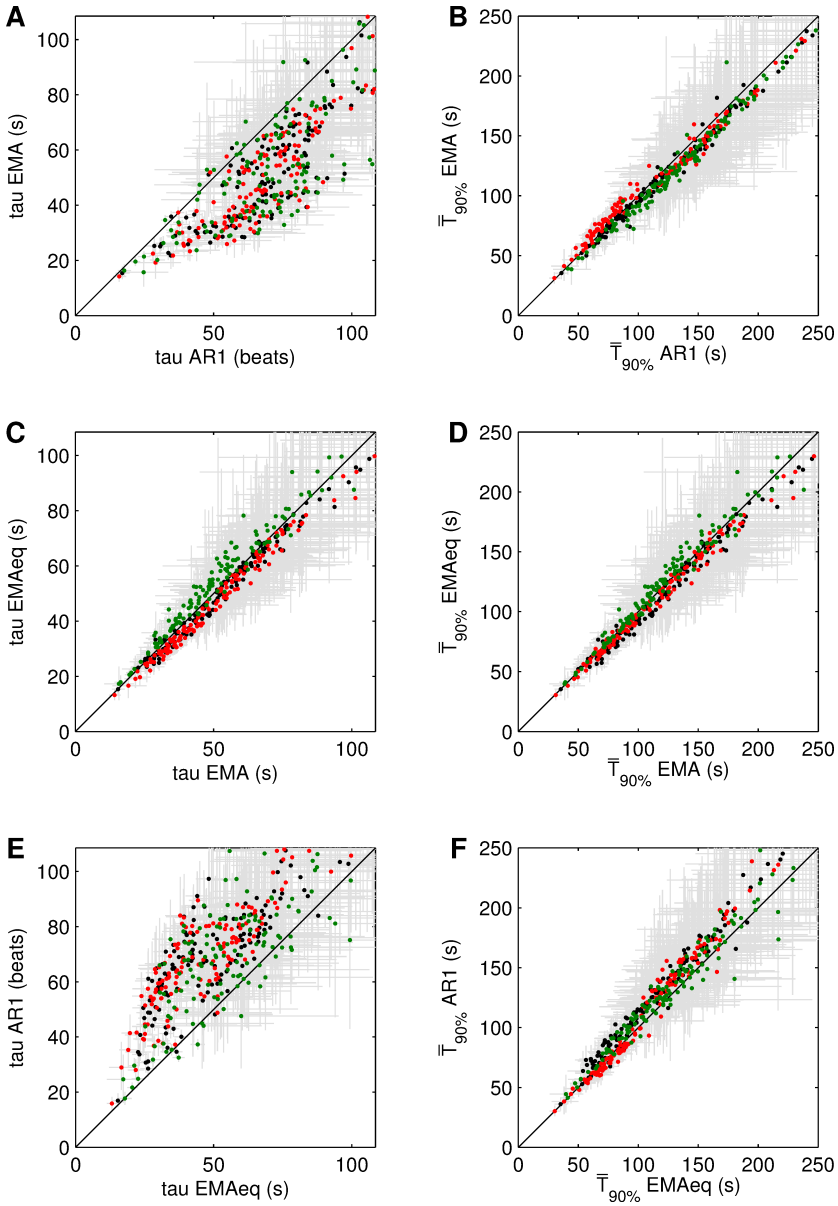

Figure 2. Comparison of the methods AR1, EMA and EMAeq to estimate τ (left panels) and $\overline{T}_{0.9}$ (right panels). Red points correspond to estimates over the condition with faster heart rates (acceleration, exercise, day), green points correspond to slower fast rates (deceleration, recovery, night) and black points are estimated over the whole recording. Error bars cover the range where the root mean square error increases by < 1 %.

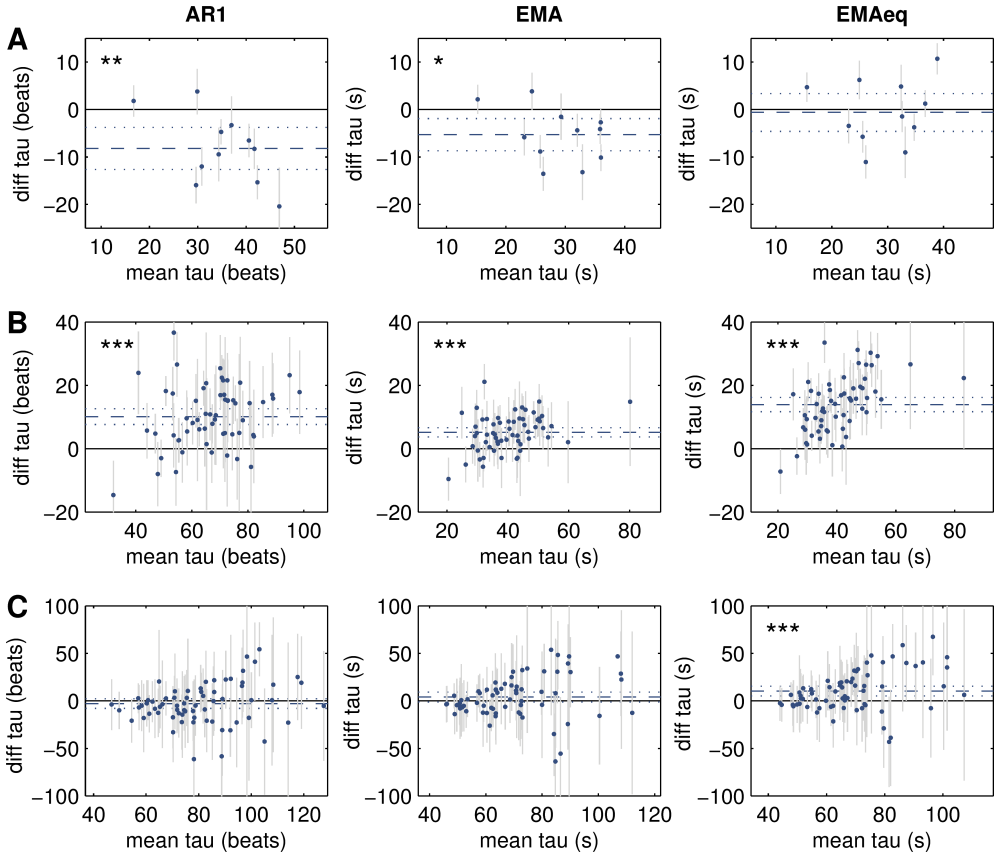

Figure 3. Bland-Altman plots of the time constant τ for the three models AR1, EMA and EMAeq representing: (A) τ(deceleration) $-$ τ(acceleration) during tilt test, (B) τ(recovery) $-$ τ(exercise), and (C) τ(night) $-$ τ(day) in Holter 24h. The length of the error bars is equal to the square root of the sum of the uncertainties of the two measures of τ. The mean (horizontal dashed line) $\pm$ 1.96 $\times$ standard error on the mean (dotted lines) are also shown. The stars refer to a paired t-test: * $p < 0.05$, ** $p < 0.01$, *** $p < 0.001$.

method caused by the slower mean heart rate during deceleration (Table 4). In contrast, during Holter 24h, the adaptation time $\overline{T}_{0.9}$ was also longer at night ($p < 0.05$) with the models AR1 and EMA. The results were preserved for the exercise protocol.

In the Bland-Altman plots of Fig. 4B, a correlation coefficient from 0.47 to 0.56 was observed, meaning that the larger the value of τ, the larger the τ difference between exercise and recovery. Using the EMAeq model, effect size, defined as the τ difference divided by τ, was found to be of the order of 33% in the exercise protocol, and 13% between days and nights.

4. Discussion and conclusion

We studied three models of QT hysteresis (AR1, EMA and EMAeq). The lag-based model AR1 has a time constant in beats, an exact exponentially decreasing weight (impulse response) and an exact exponential adaptation to an abrupt change in heart

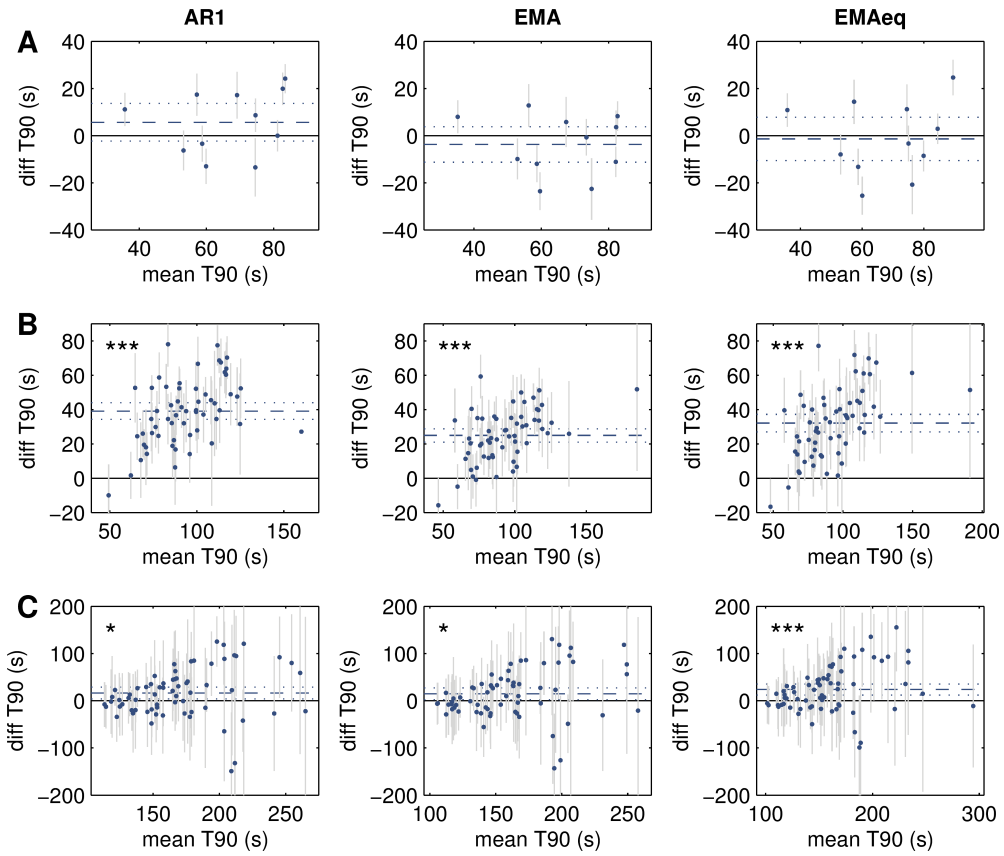

Figure 4. Bland-Altman plots of the time constant $\overline{T}_{0.9}$ (T90) for the three models AR1, EMA and EMAeq representing: (A) $\overline{T}_{0.9}$(deceleration) − $\overline{T}_{0.9}$(acceleration) during tilt test, (B) $\overline{T}_{0.9}$(recovery) − $\overline{T}_{0.9}$(exercise), and (C) $\overline{T}_{0.9}$(night) − $\overline{T}_{0.9}$(day) in Holter 24h. The length of the error bars is equal to the square root of the sum of the uncertainties of the two measures of $\overline{T}_{0.9}$. The mean (horizontal dashed line) ± 1.96 × standard error on the mean (dotted lines) are also shown. The stars refer to a paired t-test: * $p < 0.05$, ** $p < 0.01$, *** $p < 0.001$.

rate (step response). Since no time-based model with a time constant in seconds can combine these two properties, we had to develop a model with an exact exponential impulse response (EMA) and a model with an exact exponential step response (EMAeq). Thank to an efficient implementation exploiting recurrence formulas, computational complexity of these three models is similar. They also use the same inputs (QT and RR time series) and depend on a single parameter (the time constant).

The choice between these hysteresis models needs to be evaluated depending on the target application. The theoretical results demonstrated in this paper provide a guide for this choice. QT hysteresis models may be used for two main purposes: improving the accuracy of QT correction and extracting a physiological biomarker (a time constant).

As far as QT correction is concerned, time-based models (EMA and EMAeq) did not present any advantage over the simpler lag-based model (AR1). The differences in global goodness-of-fit (RMS error) were essentially meaningless, except in the case

of exercise test where the assumption that the time constant in beats is the same in exercise and recovery (AR1 model) led to slightly smaller RMS error (Table 2). This is consistent with the results from Malik et al. (2008). In addition, time-based models may cause a small bias in QTc because the mean of RR is not equal to the mean of $\overline{RR}$. Although this bias can be corrected to some extent (Table 3), the AR1 model does not suffer from that disadvantage. Note that ECG data in this study were from normal subjects in sinus rhythm. In the presence of arrhythmia (e.g. atria fibrillation or frequent premature ventricular contractions), drug intake (e.g. beta blockers) or diseased heart, these results may have to be reconsidered. Nevertheless, hysteresis models similar to ours have been used successfully in patients with atrial flutter (Jacquemet et al. 2014), atrial fibrillation (Pickham et al. 2012, Riad et al. 2017), depression and panic disorder (Baumert et al. 2008), during normal and abnormal pregnancy (Baumert et al. 2010), in patients at risk of torsade de pointes (Trost 2008), and in survivors of acute myocardial infarction (Smetana et al. 2004). Time-based hysteresis models may be particularly useful when heart rate variability is high, as during atrial arrhythmias (Riad et al. 2017).

When the objective is to extract a biomarker representing the time constant of QT hysteresis, the use of a time-based model becomes more valuable, notably in the situation of a QT-RR loop where the hypothesis is that the increasing and the decreasing arms of the loop are associated with a different hysteresis time constant. This requires comparing time constants in two conditions with different and not necessarily stable heart rates. The lag-based time constant can be corrected for heart rate (Fig. 2) as long as each condition can be associated with a single average heart rate (e.g. unimodal RR distribution). Despite having a time constant in seconds, the EMA model only has an approximate exponential adaptation to heart rate changes, causing a small bias in the determination of the time constant (underestimated when heart rate accelerates and overestimated when it decelerates). The EMAeq resolves that problem at the expense of a more complicated (non-monotonic) weights for the history of RR intervals.

In the clinical applications, the use of time-based models may lead to the suppression (tilt test) or apparition (day vs night) of statistically significant differences in hysteresis time constant (Fig. 3). The comparison of exercise vs recovery was however conclusive with all methods. The results were more consistent after correction of the time constants for heart rates (Fig. 4), thus providing more reliable biomarkers. It is important to remember that the corrections for AR1 and EMA rely on the assumption that the subject undergoes an abrupt transition from a condition A with stable RR to a condition B with faster or slower, but still stable RR. This might not be true in clinical applications, and may lead to a bias due to the choice for the value of the stable RR. The EMAeq method, though, does not necessitate such correction.

The uncertainties on the time constants were large with all methods (Table 2) expressing the fact that the RMS error is low for a wide range of parameter values around its optimum (Vinet et al. 2017). In the exercise test, effect size (EMAeq model) was about 33% (Fig. 4B) while uncertainty was 14% (Table 2). On the other hand,

in the day vs night comparison, effect size was about 13% and uncertainty 30% with significant dispersion in the differences (Fig. 4C). It is therefore advisable to compare the time constants for all the model variants before reaching conclusion.

The theoretical and experimental results of this paper suggest that the lag-based AR1 model is sufficient for determining QT-RR relations and the QTc interval, the time-based EMA model is preferable for studying the weights of the history of past RR intervals, and the time-based EMAeq model is more reliable for estimating the differences in hysteresis time constant in different physiological conditions. If needed, more sophisticated two-parameter QT hysteresis models (Halamek et al. 2010) may be created by combining the proposed models as building blocks. For instance, the model $\widetilde{RR}_i = f \cdot RR_i + (1-f) \cdot \overline{RR}_i$, where $0 < f < 1$ is a parameter to optimize, incorporates both an instantaneous response and a slow adaptation (Jacquemet et al. 2011, Riad et al. 2017).

Acknowledgments

Data used for this research was provided by the Telemetric and Holter ECG Warehouse of the University of Rochester (THEW), NY. This work was supported by the Natural Sciences and Engineering Research Council of Canada [NSERC grants number RGPIN-2015-05658 to V.J. and RGPIN-2014-05558 to A.V.] and by the FRQS "Groupe de Recherche en Sciences et Technologies Biomédicales."

Appendix A. Recurrence formulas

Consider the general situation of an unequally spaced signal $(t_i, x_i)_{i=1,\dots,N}$. The output $\bar{x}_i$ of an exponential moving average filter applied to this signal is written as

$$\bar{x}_i = \frac{a_i}{b_i} \ , \quad \text{where} \quad a_i = \sum_{j \le i} w_{i,j} x_j \quad \text{and} \quad b_i = \sum_{j \le i} w_{i,j} \ , \tag{A.1}$$

generalizing Eq. (3).

With the lag-based model $w_{i,j} = e^{-(i-j)/\tau_b}$, it is straightforward to verify that the following recurrence relations hold:

$$a_{i+1} = x_{i+1} + c\, a_i \tag{A.2}$$

$$b_{i+1} = 1 + c\, b_i \tag{A.3}$$

$$c \quad = e^{-1/\tau_b} \tag{A.4}$$

with the initial condition $a_1 = x_1$ and $b_1 = 1$. Note that for an infinitely long constant sequence with $x_i = x_0$, we have $a_i = x_0/(1-c)$ and $b_i = 1/(1-c)$. In order to stabilize the variations of $\bar{x}$ at the beginning of the recording, it is preferable to use the initial condition $a_1 = x_0/(1-c)$ and $b_1 = 1/(1-c)$, where x_0 may be x_1 or the average of x over the first few beats or minutes. It is equivalent to assuming that heart rate was constant

before the beginning of the recording. With that initial condition, $b_i = 1/(1-c)$ for all i and therefore

$$\bar{x}_{i+1} = a_{i+1}/b_{i+1} = (1-c)x_{i+1} + c\,\bar{x}_i \tag{A.5}$$

with the initial condition $\bar{x}_1 = x_0$, which corresponds to the autoregressive filter of order 1. This filter will be referred to as AR1.

Interestingly, as shown in the context of financial time series by Müller (1991) and by Eckner (2017), the recurrence relations can be generalized to the case of the time-based exponential filter with $w_{i,j} = e^{-(t_i - t_j)/\tau_s}$:

$$a_{i+1} = x_{i+1} + c_{i+1}\,a_i \tag{A.6}$$

$$b_{i+1} = 1 + c_{i+1}\,b_i \tag{A.7}$$

$$c_{i+1} = e^{-(t_{i+1} - t_i)/\tau_s} \tag{A.8}$$

These relations can be verified by substituting the definition of a_i and b_i, and (6) into them. The initial condition can be set to $b_1 = 1/(1-\exp(-\Delta t_0/\tau_s))$ and $a_1 = b_1 x_0$ by analogy with the lag-based approach. The parameter Δt_0 can be set to an average of $t_{i+1} - t_i$ over the first few beats of minutes. When the RR time series is filtered, $x_{i+1} = t_{i+1} - t_i$ so $\Delta t_0 = x_0$. This filter will be referred to as EMA (exponential moving average). Its output can be computed using $\mathcal{O}(N)$ operations whatever the value of the time constant τ_s, which would enable fast real-time computation in an ECG acquisition machine.

In order to create a filter that generalizes the AR1 filter using time-dependent coefficients, the EMA filter can be simplified by instantaneously adapting b_i to local changes in heart rate. Similarly to the lag-based model, we set $b_i = 1/(1-c_i)$, and, as a result,

$$\bar{x}_{i+1} = (1-c_{i+1})x_{i+1} + c_{i+1}\,\bar{x}_i \tag{A.9}$$

$$c_{i+1} = e^{-(t_{i+1} - t_i)/\tau_s} \tag{A.10}$$

with the initial condition $\bar{x}_1 = x_0$. This recurrence formula will be referred to as the EMAeq filter, as in Eckner (2017). Since the constant time series $x_i = 1$ gives $\bar{x}_i = 1$ whatever the sequence (t_i), the weights of the filter are properly normalized.

The weights associated with this recurrence formula are however not exponential. After iterative substitution of (A.9) on itself and identification with $\bar{x}_{i+1} = \sum_{j \le i} \tilde{w}_{i,j} x_j$, the normalized weights $\tilde{w}_{i,j}$ are found to be

$$\tilde{w}_{i,j} = (1-c_j) \prod_{k=j+1}^{i} c_k = \left(1 - e^{-(t_j - t_{j-1})/\tau_s}\right)\, e^{-(t_i - t_j)/\tau_s} \tag{A.11}$$

$$\approx \frac{t_j - t_{j-1}}{\tau_s}\, e^{-(t_i - t_j)/\tau_s} \tag{A.12}$$

where the approximation is valid when $t_j - t_{j-1} \ll \tau_s$ for all j. This means that the EMAeq filter gives more weight to long RR than to short RR. In a certain sense, the filtered time series $\bar{x}_i$ is an approximation of the integral

$$\bar{x}_i \approx \int_{-\infty}^{t_i} x(t) \frac{1}{\tau_s} e^{-(t_i - t)/\tau_s}\, \mathrm{d}t \tag{A.13}$$

where $x(t)$ is a continuous function interpolating the x time series and $\mathrm{d}t$ originates from $t_j - t_{j-1}$.

Appendix B. Step response of hysteresis models

Assume that the RR time series is an abrupt change in heart rate: $RR_i = RR_A$ if $i \leq 0$ and $RR_i = RR_B$ if $i > 0$. Then, $t_i = i\,RR_A$ if $i \leq 0$ and $t_i = i\,RR_B$ if $i > 0$. In this case, analytical expressions for the effective RR intervals can be derived. These expressions will be compared to the exponential adaptation formula with time constant τ

$$\overline{RR}_i^{\exp}(\tau) = RR_A \exp(-t_i/\tau) + RR_B(1 - \exp(-t_i/\tau)) \quad . \tag{B.1}$$

In the lag-based AR1 model with time constant τ_b (in beats), the evolution of $\overline{RR}$ is exponential as a function of the beat number, and therefore also as a function of time since the beats are evenly spaced for $t > 0$:

$$\overline{RR}_i^{\mathrm{AR1}} = \overline{RR}_i^{\exp}(\tau_b\, RR_B) \tag{B.2}$$

for $i \geq 0$.

The effective RR intervals in the EMA model with time constant τ_s can be written explicitly as (after some algebraic manipulations involving summation of geometric sequences)

$$\overline{RR}_i^{\mathrm{EMA}} = \frac{e_B RR_A + e_A RR_B\,(\exp(t_i/\tau_s) - 1)}{e_B + e_A\,(\exp(t_i/\tau_s) - 1)} \tag{B.3}$$

when $i \geq 0$ and where $e_k = 1 - \exp(-RR_k/\tau_s)$ for $k = A, B$. Since the time constant of QT adaptation is of the order of a minute, $RR_k \ll \tau_s$ so $e_k \approx RR_k/\tau_s$ and the formula can be simplified to an expression involving heart rates (HR)

$$\overline{HR}_i^{\mathrm{EMA}} = HR_A \exp(-t_i/\tau_s) + HR_B(1 - \exp(-t_i/\tau_s)) \tag{B.4}$$

where $\overline{HR}_i = 1/\overline{RR}_i$ and $HR_k = 1/RR_k$. Therefore in the EMA model, the heart rate and not the $\overline{RR}$ interval follows an exponential adaptation. Note that it implies that $\overline{RR}_i^{\mathrm{EMA}}$ is a weighted harmonic mean of RR_A and RR_B. Application of the weighted harmonic-geometric-arithmetic inequality and the Kantorovich inequality (Maze and Wagner 2009) shows that

$$\overline{RR}_i^{\exp}(\tau_s)\frac{4\,RR_B/RR_A}{(1 + RR_B/RR_A)^2} \;\leq\; \overline{RR}_i^{\mathrm{EMA}} \;\leq\; \overline{RR}_i^{\exp}(\tau_s) \quad . \tag{B.5}$$

According to the first inequality, the discrepancy between $\overline{RR}_i^{\mathrm{EMA}}$ and $\overline{RR}_i^{\exp}$ is bounded by a factor that is close to one if $RR_A \approx RR_B$. For example, for a jump in RR intervals from 1000 ms to 600 ms or the reverse, the ratio $\overline{RR}_i^{\mathrm{EMA}}/\overline{RR}_i^{\exp}$ varies over time between 0.938 and 1. The bounds (B.5) are actually tight.

The EMAeq model is here equivalent, for $t \geq 0$ (where RR intervals are constant), to an AR1 model with $\tau_b = \tau_s/RR_B$, which means that

$$\overline{RR}_i^{\mathrm{EMAeq}} = \overline{RR}_i^{\exp}(\tau_s) \quad . \tag{B.6}$$

Thus, in the EMAeq model, the adaptation from RR_A to RR_B and the recovery from RR_B back to RR_A are symmetric and exponential with the same time constant. Interestingly, if $RR(t)$ is defined as RR_A if $t \leq 0$ and RR_B if $t > 0$, then

$$\int_{-\infty}^{t_i} RR(t) \frac{1}{\tau_s} e^{-(t_i - t)/\tau_s} \mathrm{d}t = \overline{RR}_i^{\exp}(\tau_s) \tag{B.7}$$

which means that although the EMAeq model only approximates the integral (A.13), its step response is exactly exponential. More sophisticated models, for example based on linear interpolation of RR intervals (Eckner 2017), do not have that property.

Appendix C. Estimate of the bias

The RR time series will be assumed to follow a stationary random process with RR_i being independent and normally distributed with mean μ and variance σ^2. The objective is to calculate the bias $\mathsf{E}[\overline{RR}_i - RR_i]$, where $\mathsf{E}[X]$ is the expectation of a random variable X. Clearly, in the AR1 model, the bias is zero since the filter is linear and time-invariant. This is not the case with the EMA and EMAeq models. We are going to use the fact that if Z is a normal random variable with mean 0 and variance 1:

$$E[e^{-aZ}] = e^{a^2/2} \qquad \text{and} \qquad \mathsf{E}[e^{-aZ} Z] = -a\, e^{a^2/2} \ . \tag{C.1}$$

In the EMAeq model with time constant τ, the expectation of (A.9) becomes

$$\mathsf{E}[\overline{RR}_i] = \mathsf{E}[RR_i] - \mathsf{E}[c_i RR_i] + \mathsf{E}[c_i]\, \mathsf{E}[\overline{RR}_{i-1}] \tag{C.2}$$

since c_i and RR_{i-1} are independent. Then, the bias can be explicitly obtained using (C.1) and the stationarity $\mathsf{E}[\overline{RR}_{i-1}] = \mathsf{E}[\overline{RR}_i]$

$$\mathsf{E}[\overline{RR}_i - RR_i] = \frac{\sigma^2/\tau}{\exp\left(\frac{\mu}{\tau} - \frac{\sigma^2}{2\tau^2}\right) - 1} = \frac{\sigma^2}{\mu} + \mathcal{O}(\tau^{-1}) \tag{C.3}$$

where the approximation is valid when $\mu, \sigma \ll \tau$.

Calculations are more tedious in the EMA case with time constant τ, but can still be performed analytically. The bias can be estimated using the approximation of the expectation of a quotient (Stuard and Ord 1994)

$$\mathsf{E}\left[\frac{a_i}{b_i}\right] \approx \frac{\mathsf{E}[a_i]}{\mathsf{E}[b_i]} - \frac{\mathsf{cov}(a_i, b_i)}{\mathsf{E}[b_i]^2} + \frac{\mathsf{var}(b_i)\mathsf{E}[a_i]}{\mathsf{E}[b_i]^3} \ . \tag{C.4}$$

Using the same approach as in the EMAeq case, the different expectations are calculated in the large τ limit:

$$\tau^{-1}\, \mathsf{E}[a_i] \quad = 1 + \mathcal{O}(\tau^{-1}) \tag{C.5}$$

$$\tau^{-1}\, \mathsf{E}[b_i] \quad = \frac{1}{\mu} + \mathcal{O}(\tau^{-1}) \tag{C.6}$$

$$\tau^{-1}\, \mathsf{var}(b_i) = \frac{\sigma^2}{2\mu^3} + \mathcal{O}(\tau^{-1}) \tag{C.7}$$

$$\mathsf{cov}(a_i, b_i) \ = \ -\frac{\sigma^2}{4\mu}\left(1 - \frac{\sigma^2}{\mu^2}\right) + \mathcal{O}(\tau^{-1}) \tag{C.8}$$

As a result, the first term of (C.4) is equal to μ and the second is negligible as compared to the third one. This leads to a simple approximate formula for the bias

$$\mathsf{E}[\overline{RR}_i - RR_i] = \mathsf{E}\left[\frac{a_i}{b_i}\right] - \mu = \frac{\sigma^2}{2\tau} + \mathcal{O}(\tau^{-2}) \ . \tag{C.9}$$

To estimate the parameters μ and σ from the signals, the following formula can be derived using the same method as previously. For the AR1 model with $c = e^{-1/\tau}$,

$$\mathsf{E}[(\overline{RR}_i - RR_i)^2] = \frac{2c^2}{1+c}\sigma^2 = \sigma^2\left(1 - \tfrac{3}{2}\tau^{-1}\right) + \mathcal{O}(\tau^{-2}) \ . \tag{C.10}$$

Similarly, for the EMA model,

$$\mathsf{E}[(\overline{RR}_i - RR_i)^2] = \sigma^2 + \mathcal{O}(\tau^{-1}) \ , \tag{C.11}$$

and, for the EMAeq model

$$\mathsf{E}[(\overline{RR}_i - RR_i)^2] = \sigma^2 + \frac{\sigma^4}{\mu^2} + \mathcal{O}(\tau^{-1}) \approx \sigma^2 \ . \tag{C.12}$$

Obviously $\mu = \mathsf{E}[RR_i]$. In a practical case, the expectation is replaced by a mean over the samples.

References

Baumert M, Lambert G W, Dawood T, Lambert E A, Esler M D, McGrane M, Barton D and Nalivaiko E 2008 QT interval variability and cardiac norepinephrine spillover in patients with depression and panic disorder *Am J Physiol Heart Circ Physiol* **295**(3) H962–H968.

Baumert M, Seeck A, Faber R, Nalivaiko E and Voss A 2010 Longitudinal changes in QT interval variability and rate adaptation in pregnancies with normal and abnormal uterine perfusion *Hypertens Res* **33**(6) 555–60.

Berger R D 2003 QT variability *J Electrocardiol* **36 Suppl** 83–7.

Chattha I S, Sy R W, Yee R, Gula L J, Skanes A C, Klein G J, Bennett M T and Krahn A D 2010 Utility of the recovery electrocardiogram after exercise: a novel indicator for the diagnosis and genotyping of long QT syndrome? *Heart Rhythm* **7**(7) 906–11.

Chauhan V S, Krahn A D, Walker B D, Klein G J, Skanes A C and Yee R 2002 Sex differences in QTc interval and QT dispersion: dynamics during exercise and recovery in healthy subjects *Am Heart J* **144**(5) 858–64.

Chen X, Tereshchenko L G, Berger R D and Trayanova N A 2013 Arrhythmia risk stratification based on QT interval instability: an intracardiac electrocardiogram study *Heart Rhythm* **10**(6) 875–80.

Chen X and Trayanova N A 2012 A novel methodology for assessing the bounded-input bounded-output instability in QT interval dynamics: application to clinical ECG with ventricular tachycardia *IEEE Trans Biomed Eng* **59**(8) 2111–7.

Dobson C P, Kim A and Haigney M 2013 QT variability index *Prog Cardiovasc Dis* **56**(2) 186–94.

Dubé B, LeBlanc A, Dutoy J L, Derome D and Cardinal R 1988 *in* 'Proc. Engineering in Medicine and Biology Conference' Vol. 4 pp. 1768–1770.

Eckner A 2017 Algorithms for unevenly-spaced time series: Moving averages and other rolling operators *Working Paper,* downloaded on 08/15/2017 from http://www.eckner.com/papers .

Gao D s, Fang W y, Chiu-Man C, Kirsh J, Gross G and Hamilton R M 2007 QT hysteresis in long-QT syndrome children with exercise testing *Chin Med J (Engl)* **120**(3) 179–82.

Gravel H, Curnier D, Dahdah N and Jacquemet V 2017 Categorization and theoretical comparison of quantitative methods for assessing QT/RR hysteresis *Ann Noninvasive Electr* **22**(4) e12463.

Grom A, Faber T S, Brunner M, Bode C and Zehender M 2005 Delayed adaptation of ventricular repolarization after sudden changes in heart rate due to conversion of atrial fibrillation. A potential risk factor for proarrhythmia? *Europace* **7**(2) 113–21.

Halamek J, Jurak P, Bunch T J, Lipoldova J, Novak M, Vondra V, Leinveber P, Plachy M, Kara T, Villa M, Frana P, Soucek M, Somers V K and Asirvatham S J 2010 Use of a novel transfer function to reduce repolarization interval hysteresis *J Interv Card Electrophysiol* **29**(1) 23–32.

Halamek J, Jurak P, Villa M, Novak M, Vondra V, Soucek M, Frana P, Somers V K and Kara T 2007 Dynamic QT/RR coupling in patients with pacemakers *Conf Proc IEEE Eng Med Biol Soc* **2007** 919–22.

Hamidi S, Nadeau R, Karas M, Dubé B and LeBlanc A R 1997 QT interval dynamic adaptation *Proc. 23rd Annual Canadian Medical and Biological Engineering Conference (Toronto)* pp. 24–25.

Jacquemet V, Cassani Gonzalez R, Sturmer M, Dube B, Sharestan J, Vinet A, Mahiddine O, Leblanc A R, Becker G, Kus T and Nadeau R 2014 QT interval measurement and correction in patients with atrial flutter: a pilot study *J Electrocardiol* **47**(2) 228–35.

Jacquemet V, Dubé B, Knight R, Nadeau R, LeBlanc A R, Sturmer M, Becker G, Vinet A and Kuś T 2011 Evaluation of a subject-specific transfer-function-based nonlinear QT interval rate-correction method *Physiol Meas* **32**(6) 619.

Krahn A D, Klein G J and Yee R 1997 Hysteresis of the RT interval with exercise: a new marker for the long-QT syndrome? *Circulation* **96**(5) 1551–6.

Krahn A D, Yee R, Chauhan V, Skanes A C, Wang J, Hegele R A and Klein G J 2002 Beta blockers normalize QT hysteresis in long QT syndrome *Am Heart J* **143**(3) 528–34.

Lau C P, Freedman A R, Fleming S, Malik M, Camm A J and Ward D E 1988 Hysteresis of the ventricular paced QT interval in response to abrupt changes in pacing rate *Cardiovasc Res* **22**(1) 67–72.

Lauer M S, Pothier C E, Chernyak Y B, Brunken R, Lieber M, Apperson-Hansen C and Starobin J M 2006 Exercise-induced QT/R-R-interval hysteresis as a predictor of myocardial ischemia *J Electrocardiol* **39**(3) 315–23.

Lewis M J and Short A L 2006 Hysteresis of electrocardiographic depolarization-repolarization intervals during dynamic physical exercise and subsequent recovery *Physiol Meas* **27**(2) 191–201.

Malik M, Hnatkova K, Kowalski D, Keirns J J and van Gelderen E M 2012 Importance of subject-specific QT/RR curvatures in the design of individual heart rate corrections of the QT interval *J Electrocardiol* **45**(6) 571–581.

Malik M, Hnatkova K, Novotny T and Schmidt G 2008 Subject-specific profiles of QT/RR hysteresis *Am J Physiol Heart Circ Physiol* **295**(6) H2356–63.

Malik M, Hnatkova K, Schmidt A and Smetana P 2009*a* Correction for QT/RR hysteresis in the assessment of drug-induced QTc changes–cardiac safety of gadobutrol *Ann Noninvasive Electrocardiol* **14**(3) 242–50.

Malik M, Hnatkova K, Schmidt A and Smetana P 2009*b* Electrocardiographic qtc changes due to moxifloxacin infusion *J Clin Pharmacol* **49**(6) 674–83.

Malik M, Johannesen L, Hnatkova K and Stockbridge N 2016 Universal correction for qt/rr hysteresis *Drug Saf* **39**(6) 577–88.

Maze G and Wagner U 2009 A note on the weighted harmonic-geometric-arithmetic means inequalities *arXiv preprint arXiv:0910.0948* .

Müller U A 1991 Specially weighted moving averages with repeated application of the EMA operator *Working Paper,* Internal document UAM. 1991-10-14, Olsen & Associates, Seefeldstrasse 233, 8008 Zurich, Switzerland .

Pelchovitz D J, Ng J, Chicos A B, Bergner D W and Goldberger J J 2012 QT-RR hysteresis is caused by differential autonomic states during exercise and recovery *Am J Physiol Heart Circ Physiol* **302**(12) H2567–73.

Pickham D, Mortara D and Drew B J 2012 Time dependent history improves qt interval estimation in atrial fi brillation *J Electrocardiol* **45**(6) 556–60.

Pueyo E, Smetana P, Caminal P, de Luna A B, Malik M and Laguna P 2004 Characterization of QT interval adaptation to RR interval changes and its use as a risk-stratifier of arrhythmic mortality in amiodarone-treated survivors of acute myocardial infarction *IEEE Trans Biomed Eng* **51**(9) 1511–20.

Pueyo E, Smetana P, Laguna P and Malik M 2003 Estimation of the QT/RR hysteresis lag *J Electrocardiol* **36 Suppl** 187–90.

Riad F S, Razak E, Saba S, Shalaby A and Nemec J 2017 Recent heart rate history affects qt interval duration in atrial fibrillation *PLoS One* **12**(3) e0172962.

Sarma J S, Venkataraman S K, Samant D R and Gadgil U 1987 Hysteresis in the human RR-QT relationship during exercise and recovery *Pacing Clin Electrophysiol* **10**(3 Pt 1) 485–91.

Smetana P, Pueyo E, Hnatkova K, Batchvarov V, Laguna P and Malik M 2004 Individual patterns of dynamic QT/RR relationship in survivors of acute myocardial infarction and their relationship to antiarrhythmic efficacy of amiodarone *J Cardiovasc Electrophysiol* **15**(10) 1147–54.

Stuard A and Ord J K 1994 *Kendall's Advanced Theory of Statistics. Vol. 1. Distribution Theory* Halsted Press, New York, NY.

Trost D C 2008 A method for constructing and estimating the RR-memory of the QT-interval and its inclusion in a multivariate biomarker for torsades de pointes risk *J Biopharm Stat* **18**(4) 773–96.

Vinet A, Dubé B, Nadeau R, Mahiddine O and Jacquemet V 2017 Estimation of the QT-RR relation: trade-off between goodness-of-fit and extrapolation accuracy *Physiol Meas* **38**(3) 397.

Wong J A, Gula L J, Klein G J, Yee R, Skanes A C and Krahn A D 2010 Utility of treadmill testing in identification and genotype prediction in long-QT syndrome *Circ Arrhythm Electrophysiol* **3**(2) 120–5.

Zhang Y, Bao M, Dai M, Zhong H, Li Y and Tan T 2014 QT hysteresis index improves the power of treadmill exercise test in the screening of coronary artery disease *Circ J* **78**(12) 2942–9.